2011

Magnetocaloric effect in layered NdMn2Ge0.4Si1.6

Jianli Wang
University of Wollongong, jianli@uow.edu.au

S.J Campbell
University of New South Wales

J.M Cadogan
University of Manitoba Canada

A J Studer
ANSTO

Rong Zeng
University of Wollongong, rzeng@uow.edu.au

See next page for additional authors

Publication Details

Wang, J. L., Campbell, S. J., Cadogan, J. M., Studer, A. J., Zeng, R. and Dou, S. X. Magnetocaloric effect in layered $NdMn_2Ge_{0.4}Si_{1.6}$ (2011). Applied Physics Letters, 98 (23), 232509-1-232509-3.

Magnetocaloric Effect in Layered $NdMn_2Ge_{0.4}Si_{1.6}$

J.L. Wang[1,2,3], S.J. Campbell[1], J.M. Cadogan[4], A.J. Studer[2], R. Zeng[3] and S.X. Dou[3]

[1]School of Physical, Environmental and Mathematical Sciences, University of New South Wales, Australian Defence Force Academy, Canberra ACT 2600, Australia

[2]Bragg Institute, ANSTO, Lucas Heights, NSW 2234, Australia

[3]Institute for Superconductivity and Electronic Materials, University of Wollongong, Wollongong, NSW 2522, Australia

[4]Department of Physics and Astronomy, University of Manitoba, Winnipeg, MB, R3T2N2, Canada

A giant magnetocaloric effect has been observed in $NdMn_2Ge_{0.4}Si_{1.6}$ associated with the first-order magnetic phase transition from antiferromagnetism to ferromagnetism around T_C=36 K. The magnetic entropy change $-\Delta S_M$ and adiabatic temperature change ΔT_{ad} have been determined from magnetization and specific heat measurements (B=0-5 T) with $-\Delta S_M$ calculated by the Maxwell relation and Clausius-Clapeyron method. The values $-\Delta S_M^{max}$ =12.3 J $kg^{-1}K^{-1}$ and refrigerant capacity RC ~ 95 J/kg for ΔB = 0–2 T as derived from the Maxwell relation, together with the small hysteresis (thermal <0.5 K; magnetic field <0.1 T), indicate the potential of $NdMn_2Ge_{0.4}Si_{1.6}$ for refrigeration applications.

PACS: 75.30.Sg, 75.30.Kz, 61.05.F-, 75.60.Ej

Key words: magnetocaloric effect, magnetic phase transition, neutron diffraction, layered structure

Thermodynamic control of the magnetic moments and transition temperatures in certain magnetic materials upon application of a magnetic field - the magnetocaloric effect (MCE) – can enable reversible heating or cooling of the material. MCE-based magnetic refrigeration has several advantages due to its environmentally friendly and energy-efficient refrigeration mechanism [*e.g.* 1–3]. Recent work has focused on the search for materials which exhibit a giant MCE, thus contributing to the design and development of viable MCE-based refrigeration [e.g. 1–4]. The Maxwell relation $\Delta S_M = \int(\delta M/\delta T)dB$ shows that the entropy change ΔS_M is governed by the magnitude of $\delta M/\delta T$ [1, 2]. In practice, the search for Giant-MCE materials is usually associated with first-order magnetic transitions (FOMT) which present a large difference in magnetization between two adjacent magnetic states [1–4].

Many rare earth (R)-transition metal (TM) intermetallic compounds exhibit a giant MCE [1, 3, 4]. Among them, the RMn_2X_2 compounds with X=Si, Ge [5, 6] attract special attention due mainly to the interesting interplay between the 3d and 4f magnetism and the fact that both the magnitude of the Mn moments and the magnetic state of the Mn-sublattice are strongly dependent on the Mn–Mn interatomic distances [6–7]. The ternary RMn_2X_2 compounds have been studied extensively because of the large variety of structural and physical properties occurring in these phases [e.g. 6] with recent investigations exploring their MCE behaviour [6-8].

We have selected the $NdMn_2Ge_{2-x}Si_x$ system for investigation because, as outlined below, the ferromagnetic ordering of the Nd sublattice offers scope for simultaneous ferromagnetic ordering of the Mn sublattice [9]. This behaviour leads to pronounced changes in magnetization at the FOMT and the prospect of a large MCE. Given the large difference in the atomic radii of Si

(1.32 Å) and Ge (1.37 Å), we expect that replacement of Si by Ge in $NdMn_2Si_2$ will significantly modify the magnetic states of both the Nd and Mn sublattices [9]. Hence, based on this ability to design the overall magnetic behaviour of $NdMn_2Ge_{2-x}Si_x$ compounds, we present a detailed investigation of the magnetic structure and magnetic phase transitions in $NdMn_2Ge_{0.4}Si_{1.6}$ in this Letter. A giant MCE has been detected in $NdMn_2Ge_{0.4}Si_{1.6}$ at the first-order temperature-induced magnetic phase transition from antiferromagnetism to ferromagnetism at $T_C = 36$ K.

Polycrystalline $NdMn_2Ge_{0.4}Si_{1.6}$ was prepared by arc melting in an Ar atmosphere and annealed at 900°C for one week in an evacuated quartz tube [9]. Rietveld refinement of an x-ray diffraction pattern confirms the single-phase nature of our $NdMn_2Ge_{0.4}Si_{1.6}$ sample with the tetragonal $ThCr_2Si_2$-type structure (space group I4/mmm) [6]. Magnetization measurements were made using a Quantum Design PPMS (5-340 K; 1 mT) and a SQUID (10-60 K; 0-5 T) with the neutron powder diffraction experiments (λ=2.4173(5) Å; 6–465 K) carried out at OPAL [10].

The temperature dependence of the magnetization of $NdMn_2Ge_{0.4}Si_{1.6}$ (6–340 K; Fig. 1(a)) reveals a magnetic transition at T_C ~36 K. This change in magnetic state is confirmed by the neutron diffraction patterns (Fig. 1(b)) as indicated by the intensity variations of the magnetic contributions to the (101) and (112) reflections. Likewise, the (111) and (101) magnetic reflections up to 460 K (Fig. 1(b)), indicate the occurrence of a magnetic transition at T_N ~360 K [6]. The occurrence of these two magnetic transitions is consistent with the corresponding transitions and magnetic behaviour of $NdMn_2Si_2$ [11]. Rietveld refinements of the neutron diffraction patterns indicate that $NdMn_2Ge_{0.4}Si_{1.6}$ is paramagnetic (PM) above T_N ~360 K and that it exhibits a canted antiferromagnetic structure (AFmc) in the temperature range T_N ~360

K>T>T_C ~36 K (details will be presented elsewhere [12]). On cooling below T_C ~36 K, $NdMn_2Ge_{0.4}Si_{1.6}$ adopts a combined Fmc(Mn)+F(Nd) magnetic structure with canted ferromagnetism (Fmc) of the Mn sublattice accompanied by an additional ferromagnetic contribution F(Nd) of the Nd sublattice along the tetragonal c-axis [12].

The temperature dependence of the lattice parameters (Fig. 1(c)) reveals that below T_C~36 K, the lattice contracts significantly in the c-direction but expands in the a-direction ($\Delta a/a_0$= +0.11%; $\Delta c/c_0$= –0.16%). By comparison, slight changes of the opposite sense are noted in both the *a* and *c* lattice parameters at the onset of antiferromagnetic coupling at T_N ~360 K. As expected, above T_N the crystal expands isotropically with increasing temperature. These lattice anomalies are also noted in the temperature dependence of the unit cell volume (Fig. 1(c)) although the volume changes at T_N and T_C are less pronounced due to the opposing effects of the changes in the *a* and *c* lattice parameters. The phonon contribution to the lattice expansion (Fig. 1(c)) was evaluated from the Grüneisen relation [6, 13] using a Debye temperature θ_D=400 K [6] and extrapolated from the paramagnetic region into the magnetically ordered region. The calculated phonon contributions and the thermal variations of *a*, *c* and *V*, reveal magnetovolume effects at both transitions, suggestive of strong magnetostructural coupling (similar to that seen in $PrMn_{2-x}Fe_xGe_2$ [6] and $Dy_2Fe_{17-x}Mn_x$ [13]).

The magnetization curves of $NdMn_2Si_{1.6}Ge_{0.4}$ around T_C~36 K for increasing and decreasing fields are shown in Fig. 2(a) with the corresponding Arrott plots shown in Fig. 2(b). The Arrott plots indicate ferromagnetic behaviour for $NdMn_2Ge_{0.4}Si_{1.6}$ below 36 K (positive intercepts on the M^2 axis) and antiferromagnetic behaviour above 36 K (negative intercepts on the M^2 axis).

As mentioned above, these findings agree with the results of our neutron diffraction investigation [12]. Close inspection of the data in Fig. 2(a) reveals that above T_C~36 K the magnetization changes slope significantly at a critical field B_{crit}. For example, B_{crit} = 1.3 T at 40 K as indicated by the arrow in Fig. 2(a) with B_{crit} found to increase with temperature. These steps in the magnetization curves indicate a field-induced antiferromagnetic to ferromagnetic phase transition above T_C~36 K with the negative slope of the Arrott plots above 36 K in Fig. 2(b) demonstrating the first-order nature of this metamagnetic phase transition.

As is evident from Fig. 2(a), the magnetic hysteresis around the AF to F transition at 36 K is less than 0.1 T while the thermal hysteresis near 36 K is less than 0.5 K (see Figs. 1(a) and 2(a)). These hysteresis values are relatively small compared to those encountered in typical materials that exhibit a giant MCE. For example, near the magnetic transition temperatures in $Gd_5Ge_2Si_2$ (~276 K) the magnetic hysteresis is ~ 1 T and the thermal hysteresis is ~2 K [1] while for $Fe_{0.49}Rh_{0.51}$ the thermal hysteresis is even larger (~10–12 K around T_C~315 K).

The isothermal entropy change, corresponding to a magnetic field change ΔB (from zero field) was derived from the magnetization data using the Maxwell relation [1–3]:

$$\Delta S_M(T,B) = \int_0^B \left(\frac{\partial M(T,B)}{\partial T}\right)_B dB \qquad (1).$$

Use of the Maxwell relation in determining ΔS_M from FOMTs has been discussed thoroughly in the literature [e.g. 1, 3, 14-19]; this has led to deep insight to the suitability of different experimental and related analytical approaches in order to establish the isothermal entropy change. Giguère *et al.* [15] noted that the Maxwell relation overestimated the entropy change at a FOMT and that the Clausius-Clapeyron equation ($\Delta S = -\Delta M(\Delta B/\Delta T)$) leads to the correct entropy

values while Casanova *et al.* [16] demonstrated the equivalence of the two approaches provided the former is evaluated within the transition region and that the maximum applied field is high enough to complete the transition. Further, Tocado *et al.* [17] demonstrated that application of the Maxwell relation to path dependent metastable thermodynamic functions (associated, for example, with hysteresis effects at a first-order transition) contributes to errors in $-\Delta S_M$. In their comprehensive investigation of different materials using different magnetization measurement processes, Caron *et al.* [18] outlined the circumstances in which $-\Delta S_M$ can be determined from the Maxwell relation, even in the case of FOMTs with thermal hysteresis. The Maxwell relation Eqn. (1), while not strictly applicable at an ideal first order transition for which $\partial M/\partial T$ is infinite, is nonetheless generally applied to real materials for which $\partial M/\partial T$ is usually finite [19]. As below, we have determined $-\Delta S_M$ values from the Maxwell relation and the Clausius-Clapeyron equation. Here, we use the $-\Delta S_M$ values derived from the Maxwell relation as a convenient MCE figure-of-merit for comparison with $-\Delta S_M$ values calculated in a similar way for other materials.

The isothermal magnetic entropy changes $-\Delta S_M(T,B)$ for $NdMn_2Ge_{0.4}Si_{1.6}$ around T_C~36 K are shown for increasing and decreasing magnetic fields in Fig. 3(a). The equivalence of the MCE values for both increasing and decreasing fields is consistent with the small thermal and field hysteresis effects noted above (Figs. 1 and 2), and indicates the reversibility of the magnetic states in field cycling experiments. The maximum values $-\Delta S_M^{max}$ determined for different field changes, ΔB, around T_C ~ 36 K are $-\Delta S_M^{max}$ = 5.4 J kg^{-1} K^{-1}, 12.3 J kg^{-1} K^{-1}, 15.3 J kg^{-1} K^{-1}, 17.4 J kg^{-1} K^{-1} and 18.4 J kg^{-1} K^{-1} for ΔB = 0–1 T, 0–2 T, 0–3 T, 0–4 T and 0–5 T, respectively. For the relatively small field change ΔB = 0–2 T, the magnetic entropy value for $NdMn_2Ge_{0.4}Si_{1.6}$ of $-\Delta S_M^{max}$= 12.3 J kg^{-1} K^{-1} is larger than that reported for Gd (5.1 J kg^{-1} K^{-1}) and close to the

value reported for $Gd_5Si_2Ge_2$ (14.1 J kg^{-1} K^{-1}) [1]. Combined with the small thermal and field hysteresis around T_C ~ 36 K, the entropy change $-\Delta S_M^{max}$= 12.3 J kg^{-1} K^{-1} for ΔB = 0–2 T indicates the potential of $NdMn_2Ge_{0.4}Si_{1.6}$ for refrigeration applications in this temperature region. The $-\Delta S_M$ values calculated from the Clausius-Clapeyron equation are also shown in Fig. 3(a) and found to be consistent with the $-\Delta S_M$ values derived from the Maxwell relation, exhibiting behaviour similar to that reported, for example, for $Gd_5Si_{1.8}Ge_{2.2}$ [16].

The magnetic entropy $\Delta S_M(T,B)$ has also been derived from calorimetric measurements of the field dependence of the heat capacity [1–3]:

$$\Delta S_M(T,B) = \int_0^T \frac{C(T,B)-C(T,0)}{T} dT \qquad (2).$$

$C(T,B)$ and $C(T,0)$ are the values of the heat capacity measured in field B and zero field, respectively. The corresponding adiabatic temperature change, ΔT_{ad}, can then be evaluated using $\Delta S_M(T,B)$ and the zero field heat capacity data as [1]: $\Delta T_{ad}(T,B) = \int_0^B \frac{T}{C_{B,P}} \left(\frac{\partial M}{\partial T}\right)_B dB$. Fig. 3(b) shows the set of heat capacity measurements obtained for $NdMn_2Ge_{0.4}Si_{1.6}$ with B=0 T, 1 T, 2 T and 5 T and the corresponding $\Delta S_M(T,B)$ (Fig. 3(a)) and ΔT_{ad} values (Fig. 3(c)). The peak values of the adiabatic temperature change are ΔT_{ad}^{max} = 2.1 K for ΔB=0–2 T and ΔT_{ad}^{max}=4.1 K for ΔB=0–5 T. As shown by Fig. 3(a), the entropy changes derived for $NdMn_2Ge_{0.4}Si_{1.6}$ from the heat capacity measurements are in good overall accord with those determined from the magnetic measurements within the experimental errors involved in these measurements [1].

The refrigerant capacity RC, defined as the product of $-\Delta S_M^{max}$ and the full width at half maximum of the $-\Delta S_M$(T) curve [1, 2], also serves as a useful indicator of the potential capability

of materials for cooling purposes. For $NdMn_2Ge_{0.4}Si_{1.6}$, RC ~ 284 J kg^{-1} and ~ 95 J kg^{-1} for field changes ΔB = 0–5 T and 0–2 T, respectively. As summarised below, the MCE values for $NdMn_2Ge_{0.4}Si_{1.6}$ compare well with those derived from magnetization data using the Maxwell relation for materials over the temperature range ~4-40 K [20-25]. Examples of materials that exhibit large MCE values for ΔB = 0–5 T are: $ErRu_2Si_2$ (T_N~5.5 K), $-\Delta S_M$ - 17.6 J kg^{-1} K^{-1} and RC = 262 J kg^{-1} [20]; Gd_2PdSi_3 (T_N~21 K) $-\Delta S_M$~11.8 J kg^{-1} K^{-1} [21]; $ErNi_5$ (T_C~10 K) $-\Delta S_M$~15 J kg^{-1} K^{-1} and RC~95 J kg^{-1} [22]; $Dy_{53.8}Co_{17.3}Al_{28.9}H_x$ around 7 K $-\Delta S_M$~11.3 J kg^{-1} K^{-1} and RC~310 J kg^{-1} [24]; DySb (T_N~11 K) $-\Delta S_M$~11.3 J kg^{-1} K^{-1} and RC~310 J kg^{-1}; $TbCoC_2$ (T_C~28 K) $-\Delta S_M$~15.7 J kg^{-1} K^{-1} and RC~354 J kg^{-1}. With $-\Delta S_M^{max}$=18.4 J kg^{-1} K^{-1} and RC~284 J kg^{-1} around T_C ~36 K, $NdMn_2Ge_{0.4}Si_{1.6}$ compares favourably with the range of materials reported to exhibit a giant MCE in this temperature region.

In summary, a giant MCE associated with the field-induced FOMT from antiferromagnetism to ferromagnetism has been observed around T_C~36 K in $NdMn_2Ge_{0.4}Si_{1.6}$. As discussed above, the giant MCE values derived using the Maxwell relation are comparable with or larger than those reported for materials that exhibit a giant MCE in the range ~4–40 K. In particular the giant MCE value $-\Delta S_M{}^{max}$ = 12.3 J kg^{-1} K^{-1} (ΔB = 0–2 T), together with the small values of thermal hysteresis (<0.5 K) and magnetic hysteresis (<0.1 T), indicate that $NdMn_2Si_{1.6}Ge_{0.4}$ is a promising candidate for application as a magnetic refrigerant in the low temperature range required for hydrogen liquefaction. This investigation also demonstrates the potential for exploration of further novel materials that exhibit a giant MCE by tuning the magnetic phase transitions in RMn_2X_2 and related layered intermetallic compounds, through chemical substitution to vary the unit cell parameters, thereby modifying the interlayer Mn–Mn spacing.

Acknowledgements

This work is supported by the ARC, AINSE and the joint agreement between UNSW@ADFA and ANSTO. JMC is supported by the NSERC and the Canada Research Chairs programme.

Reference

[1] V. K. Pecharsky and K. A. Gschneidner, Jr., *Phys. Rev. Lett*. **78**, 4494 (1997); K. A. Gschneidner, Jr., V. K. Pecharsky and A. O. Tsokol, *Rep. Prog. Phys*. **68**, 1479 (2005); K.A. Gschneidner, Jr. and V.K. Pecharsky, Int. J. Refrigeration **31**, 945 (2008).

[2] O. Tegus, E. Brück, K. H. J. Buschow and F. R. de Boer, *Nature (London)* **415**, 150 (2002); E. Brück, J. Phys. D: Appl. Phys. **38**, R381 (2005).

[3] J.D. Zou, B.G. Shen, B. Gao, J. Shen and J.R. Sun, Adv. Mater. **21**, 693 (2009).

[4] M.D. Kuz'min and M. Richter, Phys. Rev. B **76**, 092401 (2007).

[5] A.M. Tishin, J. Adv. Mater. **1**, 403 (1994).

[6] J.L. Wang, S.J. Campbell, A.J. Studer, M. Avdeev, R. Zeng and S.X. Dou, J. Phys.: Condens. Matter **21,** 124217 (2009).

[7] P. Kumar, K. G. Suresh, A. K. Nigam, A. Magnus, A. A. Coelho and S. Gama, Phys. Rev. B **77**, 224427 (2008).

[8] J.L. Wang, S.J. Campbell, R. Zeng, C.K. Poh, S.X. Dou and S.J. Kennedy, J. Appl. Phys. **105**, 07A909 (2009); R. Zeng, S.X. Dou, J.L. Wang and S.J. Campbell, J. Alloys Compd. **509**, L119 (2011).

[9] Y.G. Wang, F.M. Yang, C.P. Chen, N. Tang and Q.D. Wang, J. Appl. Phys. **81**, 7909 (1997); J.L. Wang, S.J. Campbell, J.M. Cadogan, A.J. Studer, R. Zeng and S X Dou, J. Phys.: Conf. Ser. (in press 2011).

[10] Andrew J Studer, Mark E. Hagen and Terrence J. Noakes, Physica B **385-386**, 1013 (2006)

[11] R. Welter, G. Venturini, D. Fruchart and B. Malaman, J. Alloys Compd., **191,** 263 (1993).

[12] J.L. Wang, S.J. Campbell, J.M. Cadogan, A.J. Studer, R. Zeng and S X Dou, unpublished.

[13] J.L. Wang, S.J. Campbell, O. Tegus, C. Marquina and M.R. Ibarra, Phys. Rev. B **75,** 174423 (2007) .

[14] W.B. Cui, W. Liu and Z.D. Zhang, Appl. Phys. Lett. **96**, 222509 (2010) and references therein.

[15] A. Giguère, M. Földeaki, B. Ravi Gopal, R. Chahine, T. K. Bose, A. Frydman and J. A. Barclay, Phys. Rev. Lett. **83**, 2262 (1999).

[16] F. Casanova, X. Batlle, A. Labarta, J. Marcos, L. Mañosa and A. Planes, Phys. Rev. B **66**, 100401(R) (2002).

[17] L. Tocado, E. Palacios and R. Burriel, J. Appl. Phys. **105**, 093918 (2009).

[18] L. Caron, Z.Q.Ou, T.T.Nguyen, D.T.CamThanh, O.Tegus and E.Brück, J Magn. Magn. Mater. **321,** 3559 (2009).

[19] D. Bourgault, J. Tillier, P. Courtois, D. Maillard and X. Chaud, Appl. Phys. Lett. **96**, 132501 (2010).

[20] T. Samanta, I. Das and S. Banerjee, Appl. Phys. Lett. **91**, 152506 (2007).

[21] E.V. Sampathkumaran, I. Das, R. Rawat and S. Majumdar, Appl. Phys. Lett. **77**, 418 (2000).

[22] P.J. von Ranke, M.A. Mota, D.F. Grangeia, A.M.G. Carvalho, F.C.G. Gandra, A.A. Coelho, A. Caldas, N.A. de Oliveira and S. Gama, Phys. Rev. B **70**, 134428 (2004).

[23] H. Fu, M. Zou and N.K. Singh, Appl. Phys. Lett. **97**, 262509 (2010).

[24] W. J. Hu, J. Du, B. Li, Q. Zhang and Z. D. Zhang, Appl. Phys. Lett. **92**, 192505 (2008).

[25] B. Li, W. J. Hu, X. G. Liu, F. Yang, W. J. Ren, X. G. Zhao and Z. D. Zhang, Appl. Phys. Lett. **92**, 242508 (2008).

Figure Captions

Fig. 1 (a) Temperature dependences of the magnetization for $NdMn_2Ge_{0.4}Si_{1.6}$ over the range 5–340 K as measured in a magnetic field of 1 mT (warming and cooling after first cooling in zero field). (b) Representative neutron diffraction patterns over the temperature range 15–465 K at 15 K intervals (λ = 2.4173(5) Å) and (c) The variations in lattice parameter *a*, *c* and unit cell volume *V*. The dashed lines in (c) represent the phonon contribution to the thermal expansion (θ_D = 400 K).

Fig. 2 (a) Magnetization curves for $NdMn_2Ge_{0.4}Si_{1.6}$ at the temperatures indicated (32 K; 36 K to 58 K in 2 K increments) for increasing and decreasing fields (0-5 T). The hysteresis at T=44 K is indicated by the arrows and the lines are visual guides. The vertical arrow indicates the B_{crit} value at 40 K as an example;

(b) Arrott plots of M^2 versus B/M.

Fig. 3 (a) Temperature dependence of the isothermal magnetic entropy change $-\Delta S_M(T, B)$ for $NdMn_2Ge_{0.4}Si_{1.6}$ calculated from magnetization isotherms (closed symbols for increasing field and solid lines for decreasing field) and the heat capacity (open symbols). The $-\Delta S_M$ values were calculated using the Maxwell relation and the Clausius-Clapeyron equation (star symbols);

(b) the heat capacity of $NdMn_2Ge_{0.4}Si_{1.6}$ over the temperature range 4.2–80 K in magnetic fields of 0 T, 1 T, 2 T and 5 T (open symbols; the dashed lines represent guides to the eye);

(c) the adiabatic temperature change, ΔT_{ad}, calculated from the heat capacity measurements of Fig. 3(b). The lines are visual guides.

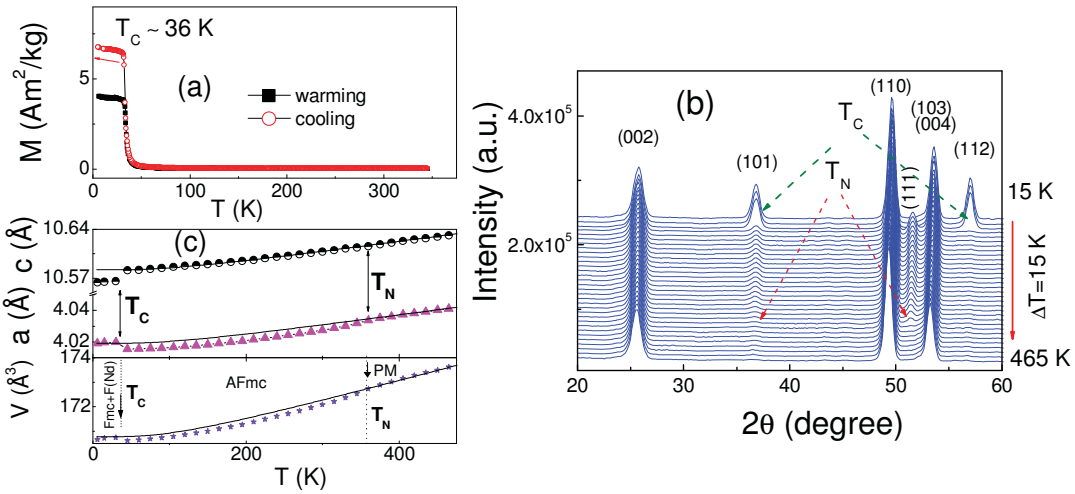
T_C ~ 36 K
(a)
warming
cooling
M (Am²/kg)
T (K)
(c)
T_N
T_C
AFmc
PM
Fmc+F(Nd)
V (Å³) a (Å) c (Å)
(b)
(002)
(101)
(110)
(103)
(004)
(112)
(111)
15 K
ΔT=15 K
465 K
Intensity (a.u.)
2θ (degree)

Fig. 1

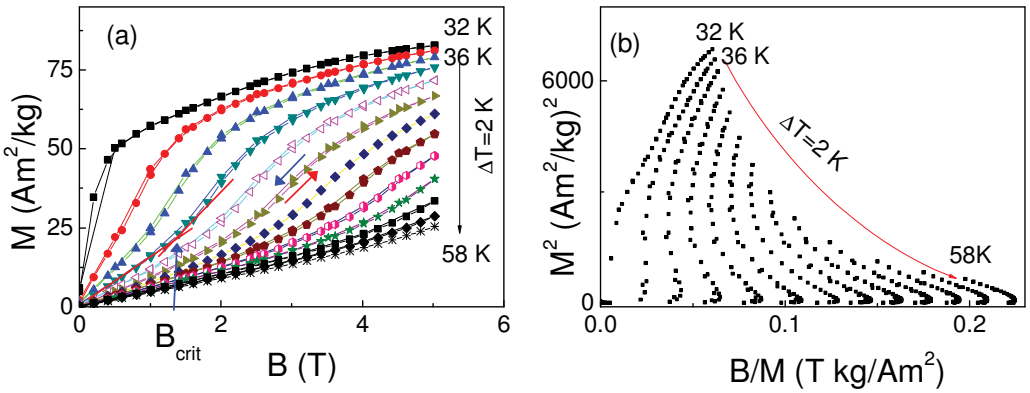
(a)
32 K
36 K
ΔT=2 K
58 K
M (Am²/kg)
B (T)
B_crit
(b)
32 K
36 K
ΔT=2 K
58K
M² (Am²/kg)²
B/M (T kg/Am²)

Fig. 2

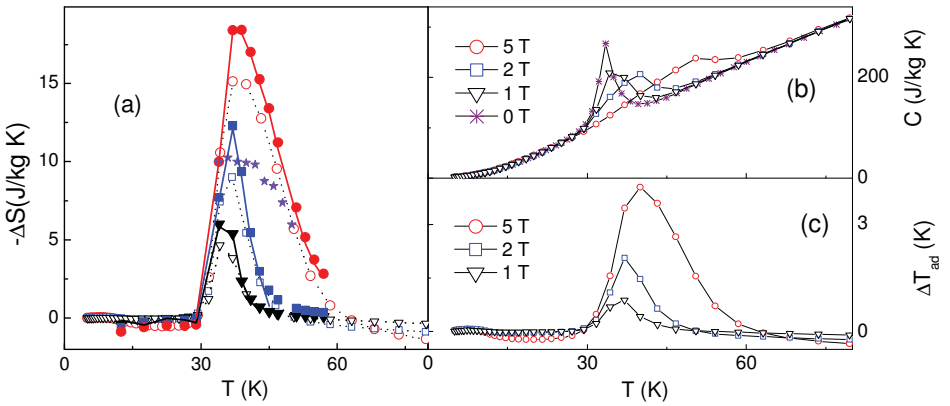

Fig. 3